Intrusion location technology of Sagnac distributed fiber optical sensing system based on deep learning

Jinyi Wu, Rusheng Zhuo, Shengpeng Wan, Xinzhong Xiong, Xinliang Xu, Bin Liu, Juan Liu, Jiulin Shi, Jizhou Sun, Xingdao He, Qiang Wu

***Abstract*—For distributed fiber optical sensing based on Sagnac effect, the intrusion is usually located by notch frequency. However, the notch spectrum is the comprehensive result of the intrusion, so when multiple disturbances simultaneously intrude from different positions of the sensing fiber, it is impossible to establish a mathematical expression between the intrusion position and the notch frequency, this leads to the problem of multi-point intrusion localization. Therefore, in this paper, deep learning technology is used to locate multiple disturbing points in Sagnac distributed optical fiber sensing system, and the related specific technologies of deep learning appling to sagnac distributed optical fiber sensing are studied. First, according to the characteristics of the system, a network structure based on the regression probability distribution is proposed, second, a loss function is constructed. The results show that the trained model can realize the positioning of multiple and single intrusion points.**

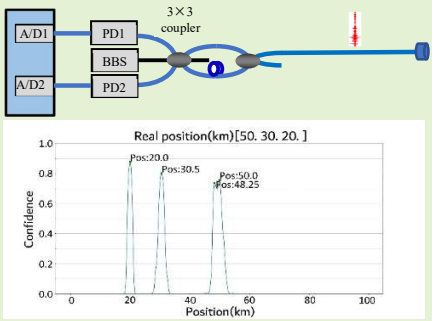

***Index Terms*—Fiber optical sensor, Sagnac interferometers, position measurement, deep learning**

I. Introduction

Fiber optical vibration sensor can be applied to pipe intrusion, pipeline leakage, perimeter security, structural health (including bridges, tunnels, slopes, railways and so on.), cable partial discharge, and intelligent wear, etc., is being received more and more attention[1-9]. Fiber optic vibration sensor can be divided into three types: point sensor[1-4], quasi-distributed sensor[5-6], and distributed sensor[8-9]. Compared with point fiber optical sensor, distributed fiber optical vibration sensor can measure vibration at any position, which has attracted more and more attention.

Distributed fiber optical vibration sensing mainly has two types: scattering type and interference type[9-10]. The distributed fiber optical vibration sensor based on scattering has the characteristics of high spatial resolution, but its disadvantages are obvious, such as needs high-speed data acquisition card, multiple measurements to improve SNR (signal-to-noise ratio), complex technology to improve dynamic response capability, which greatly increases the cost of the system.

The interferometric distributed fiber optical vibration sensor is mainly based on MZI effect or Sagnac effect. The distributed fiber optical vibration sensing technology based on MZI needs a narrow linewidth light source, which improves the cost of the system and the requirements of the application environment, and affects the stability of the system. In order to obtain the disturbance position, a dual MZI structure is proposed[11-12], which not only increases the demand for the number of optical fibers, but also requires a reference optical fiber which is not affected by the disturbance signal, which increases the construction difficulty of the system. At the same time, in order to improve the positioning accuracy of the system, high-speed acquisition card is needed, which further increases the cost of the system. Sagnac distributed optical fiber sensor uses the interference of two beams with zero optical path difference to realize the detection of intrusion signals[13]. Therefore,

Manuscript received December 25, 2020. This work was supported in part by Natural Science Foundation of Jiangxi Province under Grant 20202ACBL202002, in part by The Academic and Technical Leader Plan of Jiangxi Provincial Major Disciplines under Grant 20172BCB22012, in part by the National Natural Science Foundation of China under Grant 61465009. (Jinyi Wu and Shenpeng Wan contributed equally to this work.) (Corresponding authors: Shengpeng Wan; Jiulin Shi.)

J.Wu, R.Zhuo, S.Wan X.Xiong, X.Xu, J.Shi, and X.He are with the National Engineering Laboratory for Nondestructive Testing and Optoelectric Sensing Technology and Application, Nanchang Hangkong University, Nanchang 330063, China (e-mail: 1181977463@qq.com; rushengfeiniu@163.com; sp_wan@163.com; 1364799257@qq.com; 1460084477@qq.com; jlshi@nchu.edu.cn; xingdaohe@126.com).

B.Liu is with the Jiangxi Engineering Laboratory for Optoelectronics Testing Technology, Nanchang Hangkong University, Nanchang 330063, China (e-mail: liubin@nchu.edu.cn).

J.Liu is with Key Laboratory of Nondestructive Testing (Nanchang Hangkong University), Ministry of Education, Nanchang Hangkong University, Nanchang 330063, China (e-mail: 18042@nchu.edu.cn).

J.Sun are with the library, Nanchang Hangkong University, Nanchang 330063, China (jz77_sun@163.com).

Q.Wu is with the Department of Mathematics, Physics and Electrical Engineering, Northumbria University, Newcastle Upon Tyne NE1 8ST, U.K., and also with the School of Physics and Optoelectronic Engineering, Nanjing University of Information Science and Technology, Nanjing 210044, China (e-mail: qiang.wu@northumbria.ac.uk).

broadband incoherent light sources can be used, which greatly simplifies the structure of the system, reduces the cost of the system, and increases the stability. At the same time, Sagnac distributed optical fiber sensor has a higher response frequency than the scattered distributed optical fiber sensor, however, when intrusions occur at multiple points at the same time, the interferometric distributed optical fiber sensor has difficulty in positioning. Of course, we think that the performance of φ-OTDR may also be affected by multi-point disturbance. Because the signal reflected from the far end will be modulated by the disturbance signal from the near end, these disturbances are also superimposed together.

In distributed Sagnac optical fiber sensor, the positioning technology mainly include notch frequency method[14-17], phase ratio method[18-20] and time correlation method[21]. Phase ratio method is to use different wavelength [18-19] or carrier [20] to construct two sets of sensor systems with unequal optical path, and to realize disturbance location by dividing the interference signals of two frequencies or wavelengths. In time correlation method[21], two independent interference optical paths are constructed, and the phase of the two optical signals is processed and then the correlation operation is performed to obtain the delay difference, so as to realize the location of the intrusion. The notch frequency location method is based on that the amplitude of the phase difference function is related to the cosine function of the product of the intrusion position and the intrusion signal frequency, so the power spectral density curve of phase difference will be equal to zero at some frequencies, which is the principle of notch frequency location. Of course, the above three methods can only realize the location of single point intrusion. Therefore, in order to realize simultaneous location of multi-point intrusion, a scheme combining Sagnac and OTDR based on pulse light is proposed in [22].

For the location method based on notch frequency, when there are intrusions at different positions of the sensing fiber at the same time, the notch frequency is not a linear addition of the notch frequencies determined by a single intrusion signal, but the result of the combined action of all intrusions location. As a result, it is impossible to establish the mathematical relationship between the intrusion position and the notch frequency. Therefore, it is difficult to locate the intrusion of the system when multiple positions are disturbed at the same time. In this letter, the location problem under multi-point intrusion is studied.

II. Theoretical Analysis

Fig.1 is the system structure of the linear Sagnac distributed optical fiber sensor. In Fig.1, BBS is Broad bandwidth source, A/D is Analog-to-digital, PD is photodetector, FRM is Faraday rotator mirror.

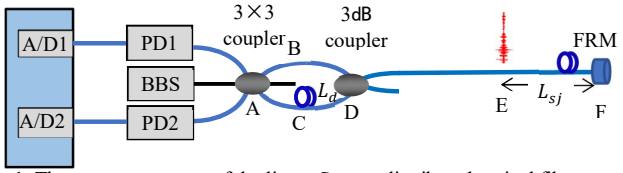

Fig.1. The system structure of the linear Sagnac distributed optical fiber sensor.

In Fig.1, there are four light routes in the system, but only two light paths with 0 optical path difference (OPD) can interfere with each other due to the very small coherent length of the broadband light source. They are

II: A-B-D-E-F-E-D-C-A

III: A-C-D-E-F-E-D-B-A

Where, The E point is the position of the j_{th} intrusion on the sensing optical fiber, the distance from E to F (the position of FRM) is recorded as intrusion position L_{sj}. Presuming j_{th} intrusion signal is

$$f_j(t) = \sum_i B_{ji}\, sin(\omega_{si} t) \tag{1}$$

Where, B_{ji} is the amplitude of frequency ω_{si}. Therefore, the phase difference caused by the j_{th} intrusion signal can be written as

$$\Delta\theta_j \propto \theta_{j2}(t) - \theta_{j3}(t) = \sum_i B_{ji}\left[sin\,\omega_{si}\left(t-\tau_{j1}\right) + sin\,\omega_{si}\left(t-\tau_{j2}\right) - sin\,\omega_{si}\left(t-\tau_{j3}\right) - sin\,\omega_{si}\left(t-\tau_{j4}\right)\right] \tag{2}$$

Where, τ_{j1} is the time of light from A through B, D to E, τ_{j2} is the time of light from a through B, D, E, F to E, τ_{j3} is the time of light from A through C, D to E, τ_{j4} is the time of light from A through C, D, E, F to E,

$$\Delta\theta_j \propto 4\sum_i B_{ij}\, cos\left(\omega_{si}\frac{nL_{sj}}{c}\right) sin\left(\frac{\omega_{si}}{2}\frac{nL_d}{c}\right)\cdot cos\left(\omega_{si}t - \frac{1}{2}\omega_{si}\tau_t\right) \tag{3}$$

Where, n is the refractive index and c is the speed of light, $L_d = \tau_{j3} - \tau_{j1}$ is the length difference between two arms of unbalanced MZI (Mach-Zehnder interferometer), at the same time, a delay fiber is added at the end of the sensing fiber to make $L_d \ll L_{sj}$. $\tau_t = \tau_{j1} + \tau_{j4}$ is the time it takes for light to travel around the sensing system.

When there is only the j_{th} intrusion, the relationship between the notch frequency and the intrusion position can be obtained from $cos\left(\omega_{si}\frac{nL_{sj}}{c}\right) = 0$, so,

$$L_{sj} = \frac{2k-1}{4}\frac{c}{nf_{sk}} \tag{4}$$

Or

$$L_{sj} = \frac{1}{2}\frac{c}{n\Delta f_s} \tag{5}$$

Where, $k = 1,2,3,\ldots$ is the order of notch frequency, $\Delta f_s = f_{s(k+1)} - f_{sk}$.

When there are only two intrusions, the phase difference can be written as follows

$$\Delta\theta \propto 4\sum_{j=1}^{2}\sum_i B_{ij}\, cos\left(\omega_{si}\frac{nL_{sj}}{c}\right) sin\left(\frac{\omega_{si}}{2}\frac{nL_d}{c}\right)\cdot cos\left(\omega_{si}t - \frac{1}{2}\omega_{si}\tau_t\right) \tag{6}$$

If these two intrusions are exactly the same, (6) can be written as

$$\Delta\theta \propto 8A\sum_i B_i cos\left(\omega_{si} n\frac{L_{s1}+L_{s2}}{2c}\right)\cdot cos\left(\omega_{si} n\frac{L_{s1}-L_{s2}}{2c}\right)\cdot sin\left(\frac{\omega_{si}}{2}\frac{nL_d}{c}\right)\cdot cos\left(\omega_{si}t - \frac{1}{2}\omega_{si}\tau_t\right) \tag{7}$$

Therefore, there will be two sets of null frequencies, which are

$$f_{s1k} = \frac{2k-1}{2n}\frac{c}{L_{s1}+L_{s2}} \tag{8}$$

$$f_{s2k} = \frac{2k-1}{2n}\frac{c}{L_{s1}-L_{s2}} \tag{9}$$

It can be seen from (8) and (9) that the notch frequency is not determined by the single-point intrusion position separately, but by the multi-point intrusion position. If the two intrusions are different, the relationship between the intrusion position and the notch frequency cannot be obtained.

For three or more intrusions, the phase difference can be written as:

$$\Delta\theta \propto 4\sum_j\sum_i B_{ij}\cos\left(\omega_{si}\frac{nL_{sj}}{c}\right)\sin\left(\frac{\omega_{si}}{2}\frac{nL_d}{c}\right)\cdot\cos\left(\omega_{si}t-\frac{1}{2}\omega_{si}\tau_t\right) \quad (10)$$

Therefore, whether the intrusion signal is the same or not, the relationship between the intrusion location and the notch frequency can't be obtained.

In these cases, how to locate the intrusion? This paper proposes a location technology based on deep learning.

III. Deep Learning Model Based On Regression Probability Distribution

Deep learning is a branch of machine learning. Using machine learning technology can solve some problems that are hard to be solved by artificial design and deterministic programs. Generally speaking, the task of machine learning is to make the machine learning system learn how to deal with samples. Samples refer to the set of quantitative features we collect from the objects and events we want the machine learning system to process.

Assuming that there is a intrusion at every point on the sensing fiber, every position is a intrusion point. Therefore, the prediction of the model should include every possible position and output the confidence level of the intrusion at that position. The confidence level can be understood as the probability of intrusion in a certain position of the sensing fiber. Obviously, those positions with high confidence level are the positions where the actual intrusion occurs. However, the intrusion location is a continuous value, it is unrealistic to estimate every possible intrusion location. So, in this paper, we establish the regression probability distribution model. The intention of this model is to try to locate the intrusion on the sensing fiber from the perspective of classification problem. Therefore, firstly, the sensing optical fiber is divided into several equal length continuous segments, and then the model is used to predict the probability of intrusion in each segment. If the probability of intrusion in a segment is obviously higher than the normal level, it is considered that there may be intrusion in this segment.

The model is a fully connected neural network with one input layer, one dropout layer, one output layer and multiple hidden layers. The input vector x of the input layer is the notch frequency extracted from the power spectrum of the phase difference function. The hidden layer is a number of fully connected layers with more neurons, the hidden layer uses function ReLU (Rectified Linear Unit) as the activation function. The output layer uses function Sigmoid as the activation function. The dropout layer was added before the output layer to prevent overfitting and increase the reliability of the model when processing unknown data.

The output vector y_{conf} of the output layer is related to the division of interval segments, and its length is equal to the number of segments. Output vector y_{conf} is a probability distribution along the sensing fiber, the length of y_{conf} is equal to the number of segments. Output vector y_{conf} contains the confidence level $conf_k$ of each segment, for example, [0.0, 0.1, 0.95, 0.05, 0.01, 0.16, 0.78, 0.01] indicates that the whole sensing fiber is divided into eight segments, and the model predicts that there is a large probability of intrusion in the third and seventh segments. The confidence level $conf_k$ is normalized by the activation function (here we use sigmoid function) of the output layer to (0,1). The label when training the model is the actual intrusion position vector $\hat{y}$, for example, [14000, 35000, 56000] indicates that there are three actual disturbed positions, and the distances from the FRM are 14km, 35km and 56km respectively. Intrusion position vector $\hat{y}$ and output vector y_{conf} are fed into a custom loss function to calculate the loss, thereby training the model.

In order to calculate the loss function, the intrusion position vector $\hat{y}$ is transformed into the probability distribution form $label_{conf}$ corresponding to y_{conf}, indicating whether there is intrusion in each segment.

The definition of $label_{conf}$ is as follows:

$$label_{conf}(k;\hat{y}) = \max_i\left(\exp\left(-2.3*\frac{[k-Segment(\hat{y}_i)]^2}{\sigma^2}\right)\right) \quad (11)$$

Where $\hat{y}_i$ is the value of the i_{th} element in the original label representing the location of the intrusion, that is, the position of the i_{th} intrusion. $Segment(\hat{y}_i)$ represents the sequence number of the interval segment corresponding to $\hat{y}_i$, and the function max () calculates the maximum value of all Gaussian distribution functions centered on $\hat{y}_i$ in the k_{th} segment.

The loss function is defined as follows:

$$Loss(y_{conf},\hat{y}) = \sum_{k=1}^{K}-\left\{\left[\alpha\cdot label_{conf}(k;\hat{y})+\beta\right]*\left[label_{conf}(k;\hat{y})-y_{conf}(k)\right]^2\right\} \quad (12)$$

In (12), the α and β parameters impose different weights on the loss of judgment errors in different segments, specifically, when the label has a larger value (that is, the segment close to the intrusion), a relatively heavier penalty is imposed when the error is judged. Because the number of disturbed segments in the training process is generally much smaller than the total number of segments, that is, the positive and negative examples are seriously imbalanced, which leads to training difficulties. The purpose of α and β is to adjust the relative punishment size when judging the positive and negative examples wrong, so as to reduce the training difficulties caused by the imbalance of the positive and negative examples. Of course, there is no absolute distinction between positive and negative examples after introducing the $label_{conf}$ in the form of probability distribution, but the model will tend to improve the prediction accuracy near the intrusion location. $y_{conf}(k)$ represents the confidence level of the k-th segment predicted by the model.

The network structure is shown in Table 1.

TABLE I
Model of Tegression Probability Distribution

Nr	Layer(Type)	Activation	Input Shape	Output Shape	Params
1	input_layer (Input)			(None, 15)	
2	dense_1 (Dense)	ReLU	(None, 15)	(None, 64)	1024
3	dense_2 (Dense)	ReLU	(None, 64)	(None, 128)	8320
4	dense_3 (Dense)	ReLU	(None, 128)	(None, 256)	33024
5	dense_4 (Dense)	ReLU	(None, 256)	(None, 512)	131584
6	dense_5 (Dense)	ReLU	(None, 512)	(None, 1024)	525312

7	dropout_1 (Dropout)		(None, 1024)(None, 1024)	0
8	output_layer (Dense)	Sigmoid	(None, 1024)(None, 400)	410000

In the data set used in this paper, each sample is the null frequency vector simulated by (10). In the data set, the null frequency vector of each sample has the same length M. When the number of notch frequencies is greater than M, the first M elements are taken as the notch frequency vector. When the number of notch frequencies is less than M, zero is added to the end of the sequence until the length of the sequence is equal to M. In the data set, if the number of actual intrusion points is N, then the length of disturbing position vector is N, if there are different numbers of intrusion points in the data set, the maximum number of intrusion points N_{max} is taken as the length of intrusion position vector, and the intrusion position vector whose length is less than N_{max} is filled with zero to N_{max}.

Before feeding the data into the deep learning model for training, the data needs to be preprocessed. Experience has shown that a normalized and evenly distributed data set can cause the loss function to converge more quickly. The samples whose input scale is obviously different from the mean value will make the sample distribution extremely uneven. First, these over-standard samples are removed from the data set, and then the vectors of the samples and labels are sorted and normalized.

The specific algorithm flow chart is shown in Fig.2.

The parameters of the distributed Sagnac optical fiber sensing system are as follows:

Sensing optical fiber length (the distance from D through E to F) $L = 100km$, fiber delay line length $L_d = 10km$, refractive index of optical fiber $n = 1.46$, the sampling rate of the system $fs = 41096Hz$.

The position of the disturbation point used by each sample is randomly generated, and its distance is uniformly distributed. According to the model shown in Table 1, the sensor fiber is divided into 400 consecutive equal-length segments. If the total length of the line is 100 km, the length of each section is 250 m.

When training the model, samples randomly generated by simulation under 20,000 sets of 2 intrusions and 35000 sets of 3 intrusions were used as data sets. After removing the samples that are not suitable for training the model (the number of notch frequencies extracted <4, accounting for about 5% of the total number of samples) and corresponding preprocessing, 80% of these samples are randomly selected as the training set, 10% is the verification set, and the remaining 10% is the test set. For the loss function during training, the custom loss function shown in (12) is used, and σ in (11) is set to 5, α in (12) is set to 0.99, and β is 0.01. When the loss function tends to be flat, the model training is completed.

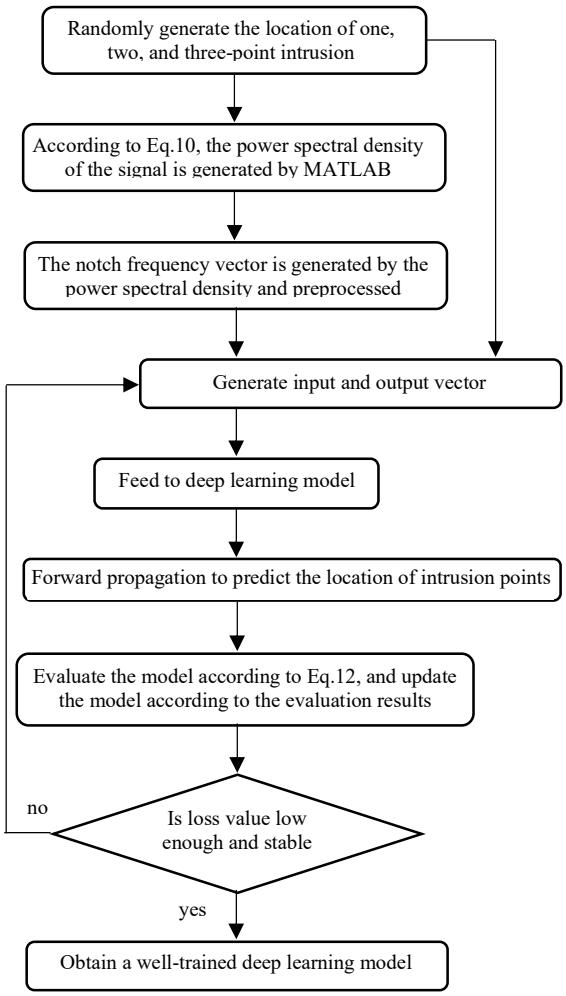

Fig.2. Algorithm flow chart

When intrusion position vector $\hat{y}$= [1.5187e4, 5.7786e4, 0e4], the power spectral density of phase difference is shown in Fig.3.

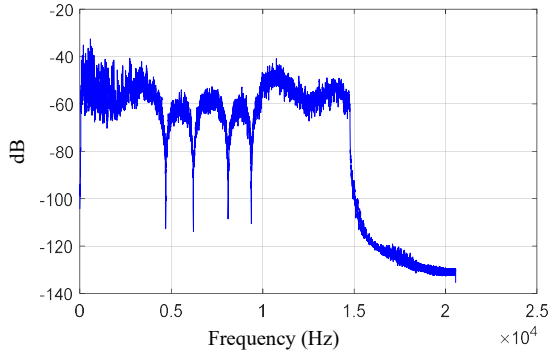

Fig.3. Power spectral density of phase difference when $\hat{y}$= [1.5187e4, 5.7786e4, 0e4]

Input the notch frequency vector obtained from Fig.3 into the trained deep learning model, and the positioning result shown in Fig.4 can be obtained, the positioning results is [1.5e4, 5.8e4, 0].

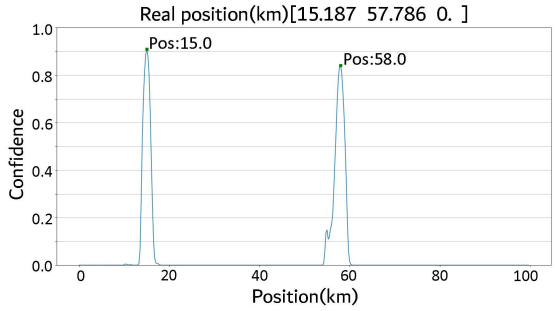

Fig.4. Positioning results output by the deep learning model when $\hat{y}$= [1.5187e4, 5.7786e4, 0e4]

When intrusion position vector $\hat{y}$ = [1.5794e4,7.1357e4,8.4351e4], the power spectral density of phase difference is shown in Fig.5.

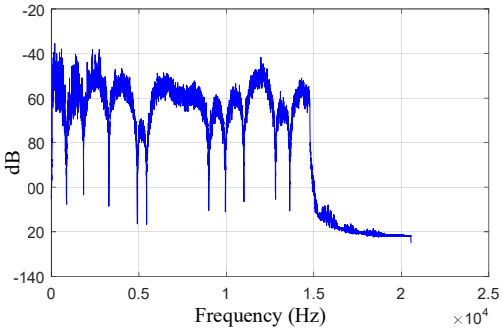

Fig.5. Power spectral density of phase difference when $\hat{y}$ = [1.5794e4,7.1357e4,8.4351e4].

Input the notch frequency vector obtained from Fig.5 into the trained deep learning model, and the positioning result shown in Fig.6 can be obtained, the positioning results is [1.55e4, 7.075e4, 8.45e4].

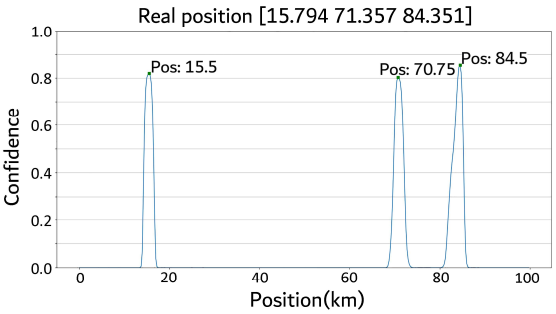

Fig.6. Positioning results output by the deep learning model when $\hat{y}$= [1.5794e4,7.1357e4,8.4351e4].

When intrusion position vector $\hat{y}$ = [3.9321e4,7.005e4,9.3482e4], the power spectral density of phase difference is shown in Fig.7.

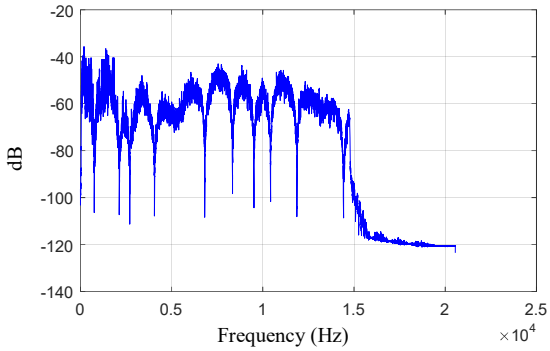

Fig.7. Power spectral density of phase difference when $\hat{y}$ = [3.9321e4,7.005e4,9.3482e4].

Input the notch frequency vector obtained from Fig.7 into the trained deep learning model, and the positioning result shown in Fig.8 can be obtained, the positioning results is [3.95e4, 6.975e4, 9.325e4].

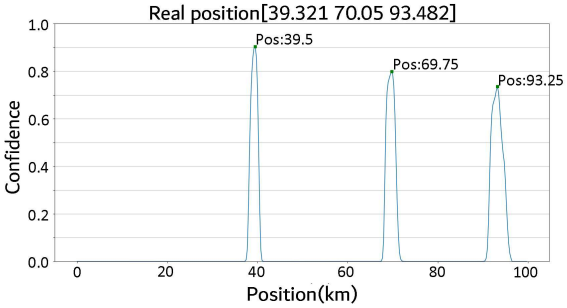

Fig.8. Positioning results output by the deep learning model when $\hat{y}$= [3.9321e4,7.005e4,9.3482e4].

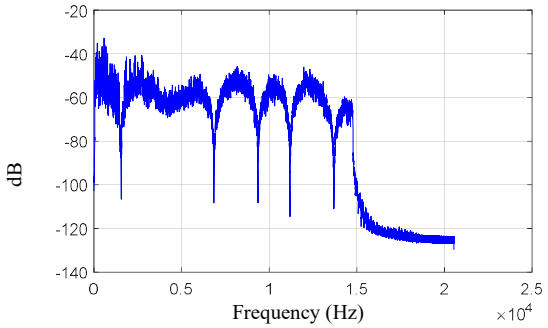

Fig.9. Power spectral density of phase difference when $\hat{y}$= [2.0e4, 3.0e4, 5.0e4].

Next, test with some data not in the test set. When intrusion position vector $\hat{y}$= [2.0e4, 3.0e4, 5.0e4], the power spectral density of phase difference is shown in Fig.9.

Input the notch frequency vector obtained from Fig.9 into the trained deep learning model, and the positioning result shown in Fig.10 can be obtained, the positioning results is [2.0e4, 3.05e4, 5.0e4] or [2.0e4, 3.05e4, 4.825e4].

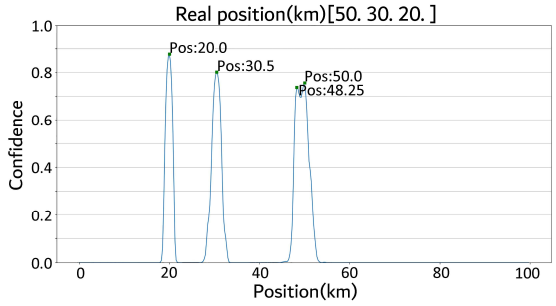

Fig.10. Positioning results output by the deep learning model when $\hat{y}$= [2.0e4, 3.0e4, 5.0e4].

When intrusion position vector $\hat{y}$= [3.0e4, 4.0e4, 5.5e4], the power spectral density of phase difference is shown in Fig.11.

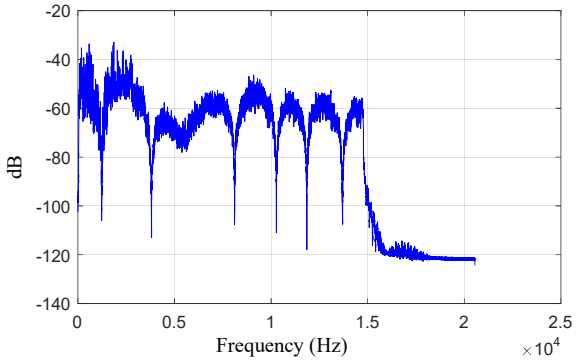

Fig.11. Power spectral density of phase difference when $\hat{y}$= [3.0e4, 4.0e4, 5.5e4].

Input the notch frequency vector obtained from Fig.11 into the trained deep learning model, and the positioning result shown in Fig.12 can be obtained, the positioning results is [2.975e4, 4.025e4, 5.55e4] or [2.975e4, 3.875e4, 5.55e4].

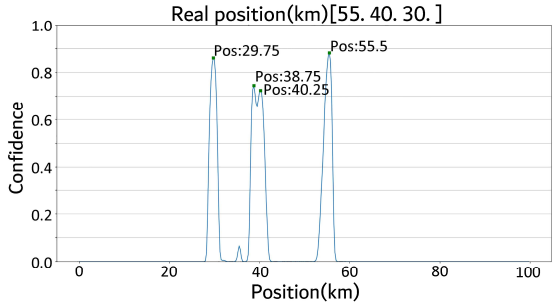

Fig.12. Positioning results output by the deep learning model when $\hat{y}$= [3.0e4, 4.0e4, 5.5e4].

Therefore, whether it is the data in the test set or the data added later, the trained deep learning model can achieve positioning.

Finally, the intrusion experiment is carried out. Because there is only one fiber stretcher, we only do a single point intrusion experiment. In the experiment, a fiber stretcher (PZ2-SMF2-APC-E produced by OPTIPHASE) is connected at about 22km away from FRM, the power spectral density of phase difference measured in the experiment is shown in Fig.13.

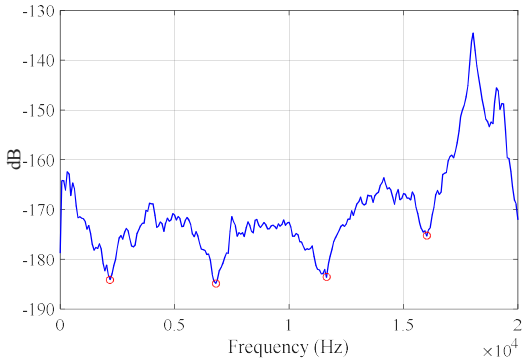

Fig.13. The power spectral density of phase difference measured by experiment.

From (5), we can get $L_s = 22.328km$. From (4), we can get $L_s = 22.669km$.

Input the notch frequency vector obtained from Fig.13 into the trained deep learning model, and the positioning result shown in Fig.14 can be obtained, the positioning results is [2.225e4, 0, 0].

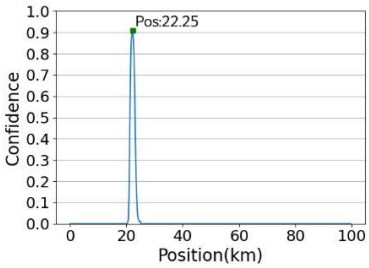

Fig.14. Positioning results output by the deep learning model when using the notch frequency vector obtained from Fig.13.

Therefore, the positioning results based on the deep learning network propsed by this paper are close to the positioning results based on notch frequency.

IV. Conclusion

Aiming at the predicament of the positioning method based on notch frequency under multi-point disturbance, this paper proposes a positioning method based on Sagnac distributed optical fiber sensing under multi-disturbance conditions based on deep learning. Aiming at the characteristics of Sagnac distributed optical fiber sensing, this paper proposes a deep learning network based on regression probability distribution model and defines the loss function of Gaussian distribution. The results show that the proposed deep learning model can realize the localization of multi-point and single point intrusion. In order to further improve the accuracy of disturbance positioning, the number of segments of the sensing fiber can be increased, but this requires a computer with better performance.

References

[1] T. Li, J. Guo, Y. Tan and Z. Zhou, "Recent Advances and Tendency in Fiber Bragg Grating-Based Vibration Sensor: A Review," IEEE Sensors Journal, vol.20, no.20, pp.12074-12087,2020.

[2] Z. Qiang, Z. Tao, H. Yusong, et al., "All-fiber vibration sensor based on a Fabry-Perot interferometer and a microstructure beam," JOSA B, vol.30, pp.1211–1215. 2013.

[3] A. G. Leal-Junior et al., "Wearable and Fully-Portable Smart Garment for Mechanical Perturbation Detection With Nanoparticles Optical Fibers," IEEE Sensors Journal, vol. 21, no. 3, pp. 2995-3003, 2021.

[4] M.Silveira M, A.Frizera, A.Leal-Junior, et al., "Transmission–Reflection Analysis in high scattering optical fibers: A comparison with single-mode optical fiber," Optical Fiber Technology, vol.58, pp.102303. 2020.

[5] A L J , R.Camilo. A.Díaz, B C M , et al., "Multiplexing technique for quasi-distributed sensors arrays in polymer optical fiber intensity variation-based sensors,". Optics & Laser Technology, vol.111,pp.81-88, 2019.

[6] A. G. Leal-Junior et al., "Quasi-Distributed Torque and Displacement Sensing on a Series Elastic Actuator's Spring Using FBG Arrays Inscribed in CYTOP Fibers," IEEE Sensors Journal, vol. 19, no. 11, pp. 4054-4061, 2019.

[7] C. Du, S. Dutta, P. Kurup, et al., "A Review of Railway Infrastructure Monitoring using Fiber Optic Sensors," Sensors and Actuators A, vol.303, pp.111728, 2020.

[8] X. Bao, D. Zhou, C. Baker and L. Chen, "Recent Development in the Distributed Fiber Optic Acoustic and Ultrasonic Detection," in Journal of Lightwave Technology, vol. 35, no. 16, pp. 3256-3267, 2017.

[9] X.Liu, B.Jin, Q.Bai, et al., "Distributed Fiber-Optic Sensors for Vibration Detection," Sensors, vol.16, pp.1164, 2016.

[10] A.D.Mcaulay, J.Wang, "A Sagnac interferometer sensor system for intrusion detection and localization," Proceedings of SPIE, vol.5435, pp.114-119, 2004.

[11] C.Ma, T.Liu, and etc., "Long-Range Distributed Fiber Vibration Sensor Using an Asymmetric Dual Mach–Zehnder Interferometers," Journal of Lightwave Technology, 34(9):2235-2239, 2016.

[12] Z.Qu, Y.Zhou, Z.Zeng, et al., "Detection of the abnormal events along the oil and gas pipeline and multi-scale chaotic character analysis of the detected signals," Measurement Science & Technology, 19(2):025301, 2008.

[13] W. Lin, "Novel distributed fiber optic leak detection system," Opt. Eng., 43(2): 278-279, 2004.

[14] J.P.Kurmer, S.A.Kingsley, J.S.Laudo, and S.J.Krak, "Distributed fiber optic acoustic sensor for leak detection," Proceedings of SPIE, vol.1586, pp.117-128, 1992.

[15] S.C.Huang, W.W.Lin, M.T.Tsai, and M.H.Chen, "Fiber optic in-line distributed sensor for detection and localization of the pipeline leaks," Sensors & Actuators A Physical, vol.135, no.2, pp.570-579, 2007.

[16] H.Wang, Q.Sun, X.Li, J.Wo, P.P.Shum, and D.Liu, "Improved location algorithm for multiple intrusions in distributed Sagnac fiber sensing system," Optics Express, vol.22, no.7, pp.7587-7597, 2014.

[17] J.Zhao, S.Pi, B.Wang, and H.Wu, "Harmonic peak locations based on the twice fast Fourier transform algorithm in a Sagnac intrusion sensing system," Applied Optics, vol.55, no.10, pp.2675-2680, 2016.

[18] J.P. Dakin, D.A.J. Pearce, A.P. Strong, et al., "A Novel Distributed Optical Fibre Sensing System Enabling Location Of Disturbances In A Sagnac Loop Interferometer," Proc Spie, 838:325-328, 1988.

[19] S.J.Spammer, P.L.Swart, A.A.Chtcherbakov, "Merged Sagnac Michelson interferometer for distributed disturbance detection," Journal of Lightwave Technology, 15(6):972-976, 1997.

[20] X.Fang, "Fiber-optic distributed sensing by a two-loop Sagnac interferometer," Optics Letters, 21(6):444-446, 1996.

[21] W. Yuan, B. Pang, J. Bo and X. Qian, "Fiber Optic Line-Based Sensor Employing Time Delay Estimation for Disturbance Detection and Location," Journal of Lightwave Technology, 32(5):1032-1037, 2014.

[22] C.Pan, X.Liu, H.Zhu, et al., "Distributed optical fiber vibration sensor based on Sagnac interference in conjunction with OTDR," Optics Express, vol.25, no.17, pp.20056-20070, 2017.

Jinyi Wu (M'2020) received the B.S. degree in Optoelectronic Information Science and Engineering from Nanchang Hangkong University, Nanchang, China in 2020.

Rusheng Zhuo received the B.S. degree in Electronic science and technology from Nanchang Hangkong University, Nanchang, China in 2014, and received the M.S. degree in optical engineering from University of Electronic Science & Technology of China, Chengdu, China, in 2018.

Sheng Peng Wan (M'93–F'2002) received the B.S. degree in physics from Nanchang University, Nanchang, China, and the Ph.D. degree in optics from University of Electronic Science & Technology of China, Chengdu, China, in 1993 and 2001, respectively. He was a post-doc at Center of Optical and Electromagnetic Research of Zhejiang University during 2003-2005. He is currently a Professor with the National Engineering Laboratory for Nondestructive Testing and Optoelectric Sensing Technology and Application, Nanchang Hangkong University, China. His current research interests include optical fiber sensors.

Xinzhong Xiong received the B.S. degree from Nanchang University, Nanchang, China. he is currently working toward the M.S. degree at Nanchang Hangkong University. His current research interests include optical fiber sensors.

Xinliang Xu is currently working toward the B.S. degree in Optoelectronic Information Science and Engineering at Nanchang Hangkong University. His current research interests include optical fiber sensors.

Bin Liu received his B.S. and Ph.D. degree from Sun Yat-sen University, China. Dr. Liu is an associate Professor with with Jiangxi Engineering Laboratory for Optoelectronics Testing Technology of Nanchang Hangkong University, China. His main research interest is fiber optic sensing.

Juan Liu received Ph.D. degree from Beijing Normal University, China. She is a lecture with Key Laboratory of Nondestructive Test (Ministry of Education) of Nanchang Hangkong University, China. Her main research interest is fiber optic sensing.

Jiulin Shi received Ph.D. degree from Huazhong University of Science and Technology, Wuhan, China. He is currently a Professor with the National Engineering Laboratory for Nondestructive Testing and Optoelectric Sensing Technology and Application, Nanchang Hangkong University, China. His current research interests include optical testing.

Jizhou Sun received the M.S. degree from Hainan University, Haikou, China.

Xingdao He received the Ph.D. degree from Beijing Normal University, Beijing, China. He is currently a Professor with the National Engineering Laboratory for Nondestructive Testing and Optoelectric Sensing Technology and Application, Nanchang Hangkong University, China. His current research interests include optical fiber sensors.

Qiang Wu received the B.S. and Ph.D. degrees from Beijing Normal University and Beijing University of Posts and Telecommunications, Beijing, China, in 1996 and 2004, respectively. From 2004 to 2006, he worked as a Senior Research Associate in City University of Hong Kong. From 2006 to 2008, he took up a research associate post in Heriot-Watt University, Edinburgh, U.K. From 2008 to 2014, he worked as a Stokes Lecturer at Photonics Research Centre, Dublin Institute of Technology, Ireland. He is with Faculty of Engineering and Environment, Northumbria University, Newcastle Upon Tyne, United Kingdom; Key Laboratory of Nondestructive Test (Ministry of Education), Nanchang Hangkong University, Nanchang 330063, China. His research interests include optical fiber interferometers for novel fiber optical couplers and sensors, nanofiber, microsphere sensors for bio-chemical sensing, the design and fabrication of fiber Bragg grating devices and their applications for sensing, nonlinear fibre optics, surface plasmon resonant and surface acoustic wave sensors. He has over 200 journal publications in the area of photonics and holds 3 invention patents. He is an Editorial Board Member of Scientific Reports, an Associate Editor for IEEE Sensors Journal and an Academic Editor for Journal of Sensors.